

Results of Aeromagnetic surveys over Volcanos and Calderas in Japan.

著者	Muroi Isao
雑誌名	Science reports of the Tohoku University. Ser. 5, Geophysics
巻	21
号	3
ページ	87-112
発行年	1973-09
URL	http://hdl.handle.net/10097/44713

Results of Aeromagnetic Surveys over Some Volcanoes and Calderas in Japan

ISAO MUROI

Department of Earth Science, Science Education Institute
of Osaka Prefecture

(Received July 24, 1972)

Abstract: Aeromagnetic surveys of the total intensity over Oshima and Hakone Volcanoes, and Towada and Onikobe Calderas in Japan were carried out at different flight levels by using a proton precession magnetometer mounted on a helicopter, in order to study their magnetic structures.

The magnetic anomaly to be measured at each height depends on the magnetic contrast of the underground structure. The rate at which the anomaly varies with the flight level is affected by the shape of the structure. From the vertical gradient of the total magnetic anomaly, the depth and shape of the structure have been determined. In Oshima, the anomaly is considerable and the structures are very complicated with several dipole models, the depth ranging from 800 m to 4 km. In Hakone, the anomaly due to the Old Somma lava is obvious. 'Kintokiyama — Maku-yama' dislocation line is made clear. Two prism-shaped models as the assumed structure for Mt. Kamiyama are considered at 0.5 and 1.0 km in depth. In the Towada district, a large low anomaly over the northeastern shore of the Lake Towada and two anomalies over Yasumiya south of the Lake were observed. The former is assumed to be a dipole with a reversed magnetization situated at 4 km in depth. In Onikobe, a caldera-like feature is shown, though the magnetic anomaly is not so considerable as the areas mentioned above.

I. Introduction

In recent years many studies have been reported on the structure of the earth, especially on the structure of the upper mantle. The studies are concentrated on common problems as to the materials of the structures, the depth of the materials and the distribution of the materials, although various methods have been adopted.

There are several methods to investigate the underground structure; the geological surveying for determining the geologic structure, the seismic measurement, gravimetric and magnetometric surveying, heat flow surveying, and electrical (including electromagnetic) exploration. These have been applied in combinations, according to the purpose of the investigation. This paper is intended to study the underground structure by aeromagnetic surveying.

In order to investigate the magnetic underground structure by the surveying, the following factors are to be known; intensity and direction of the geomagnetic field, and magnetic intensity, direction and susceptibility of the substance of the ground, and the distance to the magnetic body and its shape. Hence we must make an effort to know these factors as many as possible from direct observations. But some of the unknown factors must be assumed, because all of them can not necessarily

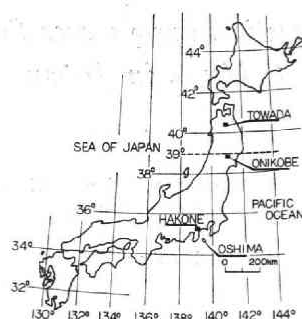


Fig. 1 Positions of the area of aeromagnetic survey.

be obtained from direct observations.

The magnetic anomaly to be measured at each height depends on the magnetic contrast of the ground. It is important to make clear how the anomaly changes with the flight level since we can estimate the shape and size of the magnetic body from the rate of the change. Then the unknown factors are decreased in number and it becomes much easier to analyze the source quantitatively.

The aeromagnetic surveys in the present paper were carried out over several volcanoes and calderas in Japan by a proton magnetometer mounted on a helicopter 'Sikolski S-55'. A total intensity of the geomagnetic field and its absolute value are directly observed by the magnetometer. The magnetic detector was towed at the end of a cable, 12 m long, attached to the bottom of the plane. At this distance, the magnetism of the plane is negligible. An intermittent camera synchronized with the frequency counting of the magnetometer was used for the determination of the flight path and the photographs were compared with a standard map to decide the observed courses. Observational error is ± 10 m in height, ± 10 m in position determined by a camera and 10~15 gammas in magnetic anomaly. The areas surveyed are Oshima, Hakone, Towada and Onikobe (Fig. 1).

2. Method of Analysis

It is generally known that there are three types of the magnetic anomaly-producing basement. These, in short, are as follows. The first is the case of intrusives due to volcanic activity. The second arises principally when the basement is uplifted and is akin to a buried horizontal cylinder. The third type is the same basement as the second one but has a horizontally finite extension and is similar to a buried sphere. The magnetic anomaly produced from such structures is given by the following relationship:

$$H = \frac{K}{r^n} \quad (1)$$

where H is the magnitude of magnetic anomaly, and K is a constant which depends on body geometry, magnetic susceptibility contrast, etc., r is the distance from a detecting element to the center of the body, and n is an exponent which depends on the

geometry of a magnetic material. The interesting feature is that n has the value 2 for a horizontal cylinder and the value 3 for a sphere.

Reviewing the basic mathematical relationship for the second and third anomaly types, the distance r can be resolved into the three cartesian coordinate directions, x and y horizontally and z vertically. Considering the partial derivative of H with respect to r it can be written as

$$x \frac{\partial H}{\partial x} + y \frac{\partial H}{\partial y} + z \frac{\partial H}{\partial z} = -nH. \quad (2)$$

This is known as Euler's relationship. The symbols x and y are the distances measured horizontally along the x and y axes, and z is a vertical distance from the center of the structure to the point at which the anomaly is measured. Along any direction x which passes over the center of the structure, y becomes zero and the second term in (2) disappears. Then Eq. (2) becomes

$$x \frac{\partial H}{\partial x} + z \frac{\partial H}{\partial z} = -nH. \quad (3)$$

Over the top of the structure, x and y are zero; at the maximum point of H ,

$\frac{\partial H}{\partial x} = \frac{\partial H}{\partial y} = 0$, and the relation can be simplified as

$$z \frac{\partial H}{\partial z} = -nH. \quad (3')$$

This can be regarded as the one-dimensional form of the potential field relationship and is most useful as a means to classify the anomalies. For convenience, H , ΔH , Z and ΔZ are displaced by other symbols; T , ΔT , h and Δh , respectively. Therefore, (3)' can be rewritten as

$$\left(\frac{\Delta T}{\Delta h} \right)_{\max} = -\frac{nT_{\max}}{h}. \quad (4)$$

This is the most basic formula for the vertical gradient of total magnetic anomaly.

1. When the total intensity anomalies obtained at two different levels h_1 and h_2 ($h_1 < h_2$) are T_1 and T_2 , respectively (Fig. 2), the vertical gradient is obtained as follows:

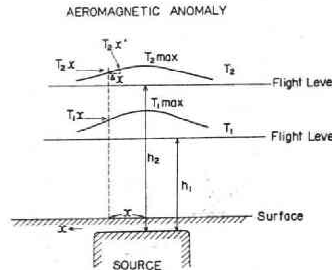


Fig. 2 Definition of the first vertical and horizontal derivatives of the total intensity at two different heights.

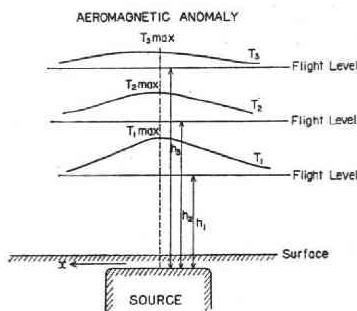


Fig. 3 Definition of the first vertical derivatives of the total intensity at three different heights.

$$\frac{\Delta T}{\Delta h} = \frac{T_2 - T_1}{h_2 - h_1}.$$

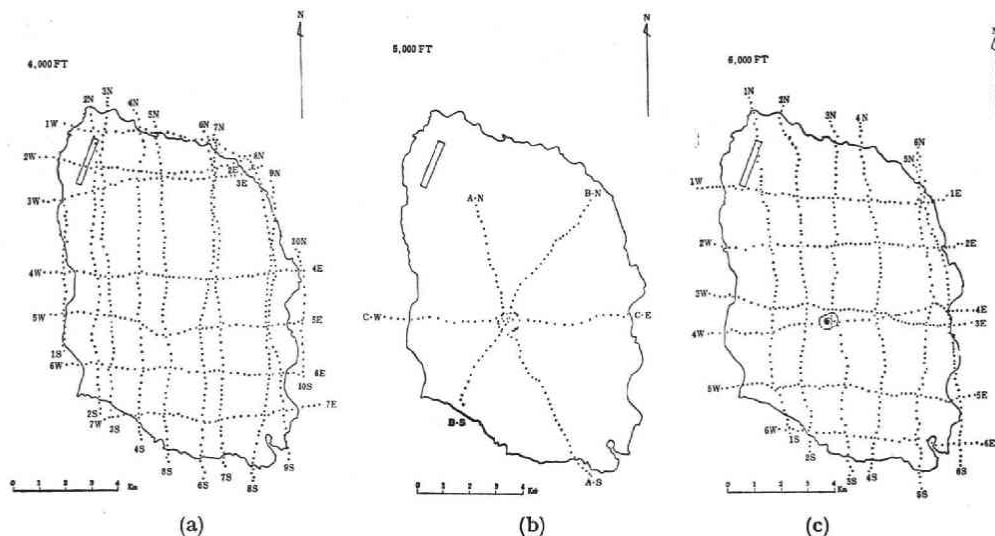
But n and h in (4) are not obtained directly. Hence in order to estimate them by Eq. (3) we need to calculate the anomaly difference ΔT between the vertical difference Δh and horizontal one Δx at the horizontal distance x from the origin. At this point, the vertical and horizontal gradients are calculated as follows:

$$\left(\frac{\Delta T}{\Delta x}\right)_x = \frac{T'_2 - T_2}{x_2 - x_1}, \quad \left(\frac{\Delta T}{\Delta h}\right)_x = \frac{T_2 - T_1}{h_2 - h_1}$$

where T'_2 is the magnitude of the anomaly at a point x_2 . From (3)

$$x \frac{T'_2 - T_2}{x_2 - x_1} + h \frac{T_2 - T_1}{h_2 - h_1} = -nT_1. \quad (5)$$

And from (4) and (5), n and h are calculated. And the intensity of the magnetization and the magnetic moment are easily determined.



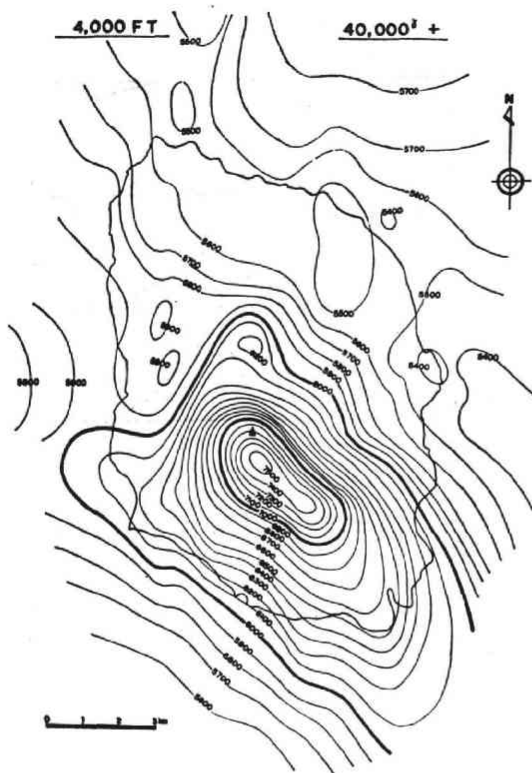


Fig. 6 Total magnetic intensity over the Oshima Volcano at 5000 ft in height.

←Fig. 5 Total magnetic intensity over the Oshima Volcano at 4000 ft in height.

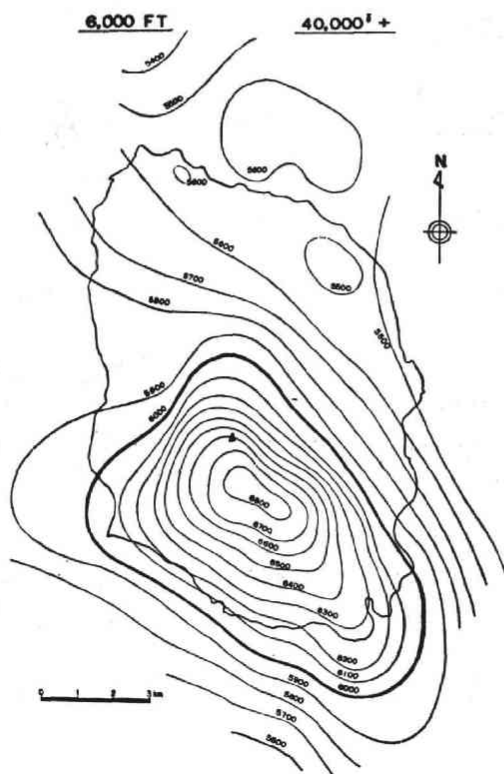


Fig. 7 Total magnetic intensity over the Oshima Volcano at 6000 ft in height.

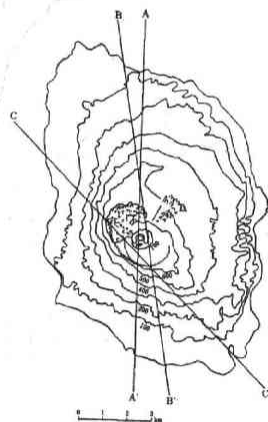


Fig. 8 Traverses of profile section of total intensity and topographic map.

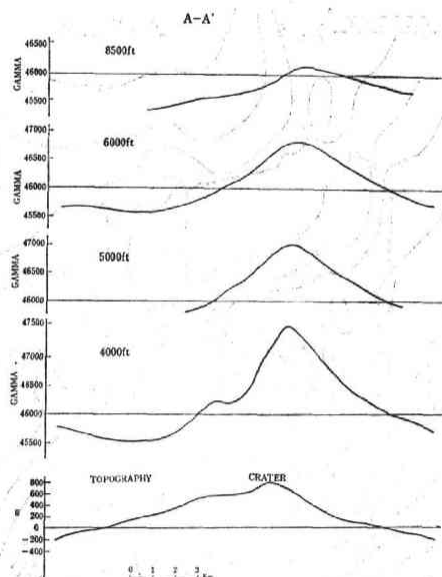


Fig. 9 Profiles of total intensity and topography (traverse A-A').

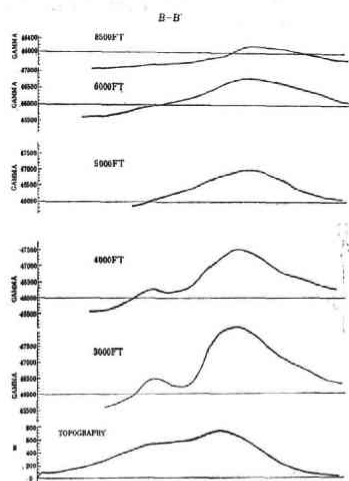


Fig. 10 Profiles of total intensity and topography (traverse B-B').

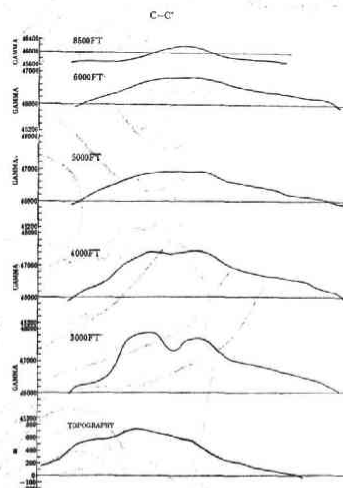


Fig. 11 Profiles of total intensity and topography (traverse C-C').

2. When three different anomalies T_1 , T_2 and T_3 are observed at three different altitudes h_1 , h_2 and h_3 ($h_1 < h_2 < h_3$, $h_2 - h_1 < h_1$, $h_3 - h_2 < h_2$) respectively, n and h are determined by an arbitrary combination of two out of the three altitudes (Fig. 3).

Several examples of the aeromagnetic surveys by the magnetic gradiometer are obtained by Whickermann (1954), Allan (1965), Hood (1965), Slack *et al.* (1967) and Hertman *et al.* (1971).

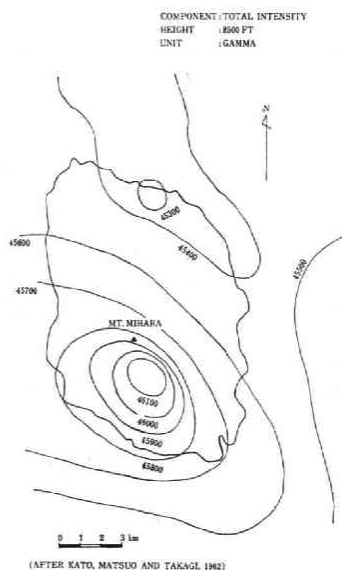


Fig. 12

Fig. 12 Total magnetic intensity over the Oshima Volcano at 8500 ft in height (after Kato, Matsuo and Takagi, 1962).

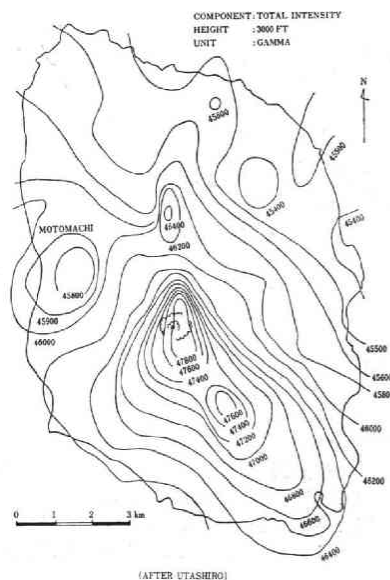


Fig. 13

Fig. 13 Total magnetic intensity over the Oshima Volcano at 3000 ft in height (after Utashiro,).

3. Aeromagnetic Surveys

3-1. Oshima Volcano

Oshima Volcano, belonging to the Fuji volcanic belt, is a typical tripple strato-volcano and is still active with the emittance of smoke. The main volcanic cone is the strato-volcano of olivine basalt, pyroxene-olivine basalt and subordinate pyroxene andesite with or without olivine phenocrysts (after Kuno *et al.*, 1962).

This volcano has been surveyed in greater detail than other ones. In order to have a better understanding of the horizontal distribution and the vertical variation of magnetic anomaly due to magnetic bodies in the underground, the magnetic anomaly was observed at three different flight levels. At these levels, 4000 ft (1220 m), 5000 ft (1520 m) and 6000 ft (1630 m), the flight courses are shown in Fig. 4. The observation points were determined from air photographs. The interval of each point is about 250 m. Magnetic maps observed are shown in Figs. 5, 6 and 7. From these maps, it is clear that (1) in the northern side of the volcano no distinct anomaly appears, but in the southern side a pronounced anomaly with a shape like a cocoon is seen from the crater of this volcano to the south-eastern marine ridge, and (2) the feature for each height is different in shape and size of the anomaly. The higher the altitude is, the simpler becomes the magnetic map.

Next, let us look at the magnetic maps from a vertical view. Several typical traverses are shown with the topography in Fig. 8. Sections A-A', B-B' and C-C' are taken in the north-south trend traversing the crater (Figs. 9, 10 and 11). The value at 8500 ft (2600 m) in height was quoted from the result observed by Kato, Matsuo and

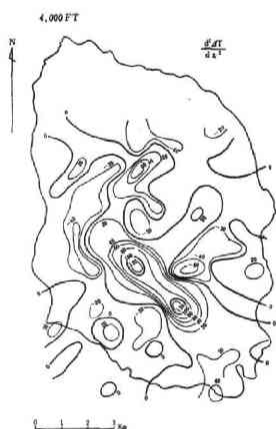


Fig. 14



Fig. 15

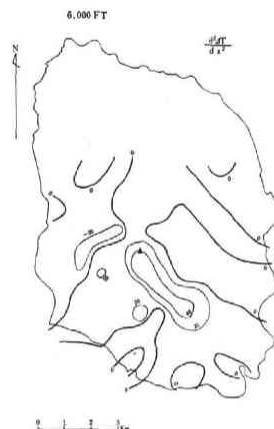


Fig. 16

Fig. 14 Second vertical derivatives at 4000 ft.
 Fig. 15 Second vertical derivatives at 5000 ft.
 Fig. 16 Second vertical derivatives at 6000 ft.

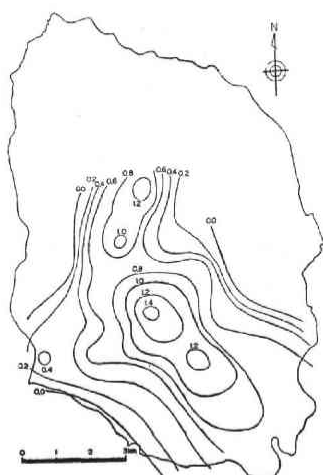


Fig. 17

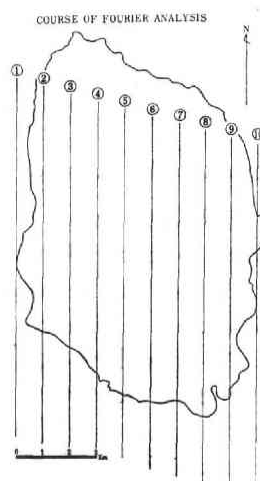


Fig. 18

Fig. 17 Vertical-gradient map calculated from total intensity at 4000 ft, 5000 ft and 6000 ft in height (Contour interval 0.1γ/ft).
 Fig. 18 Ten courses for calculating anomaly spectrum by Fourier analysis.

Takagi (Fig. 12) in 1962, using a flux-gate type magnetometer, and the value at 3000 ft (910 m) in height, by Utashiro (private communication) using a proton magnetometer (Fig. 13).

Second vertical derivatives to know the horizontal distribution of the magnetic bodies were calculated. Figs. 14, 15 and 16 show the second vertical derivatives computed by means of a formula of Henderson *et al.* (1964) from the total-field intensity. The unit is gammas per km square. These show the existence of the magnetic body with a cocoon-shape traversing the crater from northwest to southeast. Further, a vertical gradient was obtained from the total intensity at three flight levels

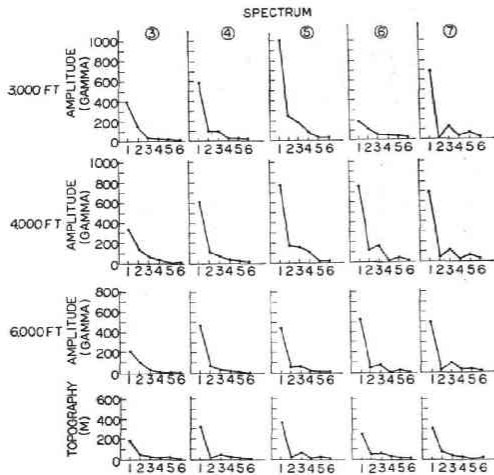


Fig. 19

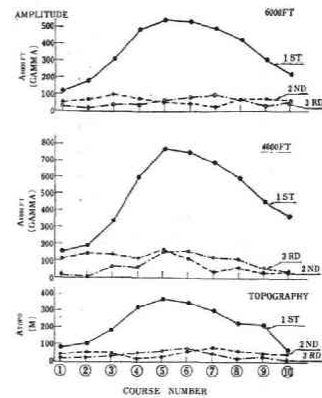


Fig. 20

Fig. 19 Anomaly spectrum of the sources ③ to ⑦ at 3000 ft, 4000 ft and 6000 ft.

Fig. 20 Anomaly amplitude to each course at 4000 ft and 6000 ft. Topographic amplitude is also shown for comparing with magnetic one.

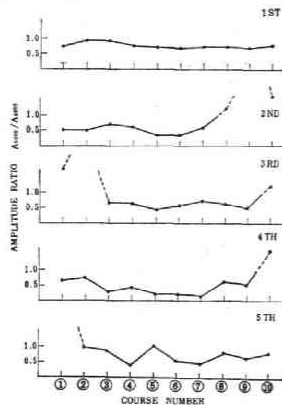


Fig. 21

Fig. 21 Amplitude ratio of anomaly at 6000 ft to that at 4000 ft.

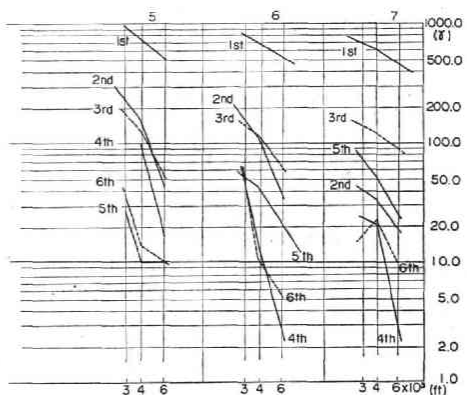


Fig. 22

Fig. 22 Variations of anomaly amplitude of each term due to different heights (3000 ft, 4000 ft and 6000 ft) concerning the course ⑤, ⑥ and ⑦.

(Fig. 17). The unit is 0.1 gamma per foot. The largest value is 1.4 near the crater.

For the purpose of quantitatively treating the magnetic anomaly distribution, the anomaly spectrum was calculated. Fig. 18 shows the ten courses of the north-south section of 13 km in length with 1 km intervals in the east-west direction. A spectrum of the topography was also calculated. Each first term is the largest as shown in Fig. 19. The amplitude of the each term of each course is shown in Fig. 20. First of all, we can find a great difference of the first term from the second one. The amplitude of the first term seems to be due to the magnetically deepest structure of this volcano. Fig. 21 shows the ratio of the amplitude at 6000 ft to that of 4000 ft. In this figure, the uppermost curve is the ratio of the first terms and the value is about 1.0 indicating

Table 1. Examples of anomaly sources.

Source	Depth of the Source (km)	Intensity ($\frac{\text{emu}}{\text{cc}}$)	Magnetic Moment (CGS. emu)
A	0.78	0.77×10^{-3}	1.6×10^{12}
B	3.63	4.82×10^{-3}	1.0×10^{14}
C	0.75	1.92×10^{-3}	3.4×10^{12}
D	0.54	1.54×10^{-3}	1.0×10^{12}
E	1.55	2.08×10^{-3}	3.2×10^{13}
F	1.25	2.05×10^{-3}	1.7×10^{13}
(G)	3.68	4.80×10^{-3}	1.0×10^{14}

(G) is the same as B.

DISTRIBUTION OF ANOMALY SOURCES

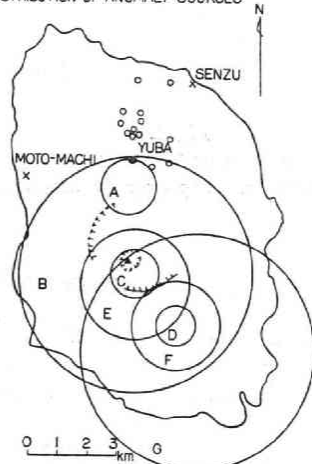


Fig. 23

Fig. 23 Anomaly sources obtained from aeromagnetic surveys at three different heights: Epicenters of earthquakes (after Takahashi and Nagata, 1939).

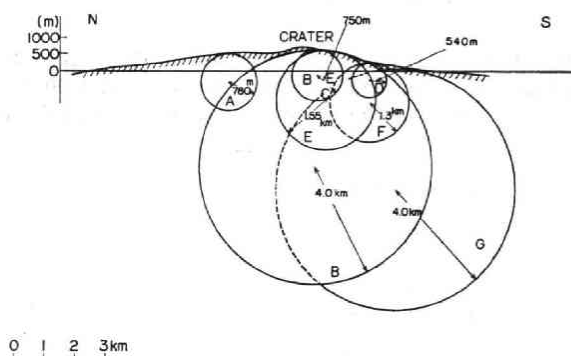


Fig. 24

Fig. 24 Vertical section of the anomaly sources.

that the change of the anomaly at the different heights is very small; the ratio of the second term is about 0.5, but it decreases to 0.3 in courses ⑤ and ⑥ near the crater. This means that the magnetic body is shallow near the crater. The third and fourth are similar. From these results, we can understand that the magnetic anomaly sources of this volcano are intricately distributed.

The magnetic anomalies were analyzed as follows. The formula (5) as stated before cannot be applied directly to the area with such complex structures as in this volcano. Then we develop the anomaly to the Fourier series and use the calculated amplitude for the following analysis. Fig. 22 shows these features to the sixth term. The upper numbers ⑤, ⑥ and ⑦ from the left show the course numbers analyzed. For the ⑤, the amplitude varies linearly with the height to the third term but its gradient differs. Each of the first terms of ⑤, ⑥ and ⑦ corresponds to the same magnetic source. Then from (5), it was assumed that the each magnetic source is a dipole. And to calculate the dipole moment and intensity of the magnetization, a formula led by Smellie (1965) was used here. The depth, magnetic intensity and dipole moment are

Table 2. Some dipole models of Oshima.

Depth (km)	Intensity ($\frac{\text{emu}}{\text{cc}}$)	Dipole moment (CGS. emu)	
1. 2.7	9.8×10^{-3}	7.1×10^{16}	Rikitake and Yokoyama et al. (1951, 1957).
2. 6.5	3.0×10^{-3}	3.5×10^{15}	Kato, Matsuo and Takagi (1962).
3. 2.2	1.4×10^{-2}	2.2×10^{18}	Kato, Matsuo and Takagi (1962).

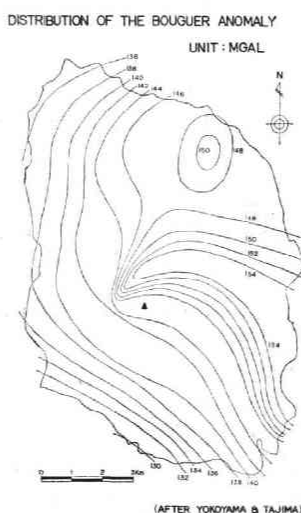


Fig. 25 Distribution of the Bouguer anomaly (after Yokoyama and Tajima, 1957).

calculated as listed in Table 1. Fig. 23 shows a horizontal distribution of the magnetic sources, and Fig. 24, its vertical section. In these figures, the dipole models B and G are considered to be the same, as in case of the models E and F. The data of B and G calculated from the different sections indicate that a source with a depth of about 4 km exists as the magnetically deepest structure in this volcano. The results of E and F mean that the magnetic formations at 1.3~1.6 km in depth exist next to the structure with a depth of 4 km as stated above. Vacquier and Uyeda (1967) ascribed the magnetic anomaly in this volcano to the topography.

Discussion

Magnetic surveys on Oshima Volcano have been made on the ground by some workers. Further, aeromagnetic surveys have been carried out by Kato, Matsuo and Takagi (1962), *et al.*. From these surveys, several dipole models are reported as shown in Table 2.

As mentioned above, the magnetic anomaly source in this volcano has been interpreted by one or two dipole models. In the present study, it was confirmed that several magnetic anomaly sources existed in this volcano. This is valuable informa-

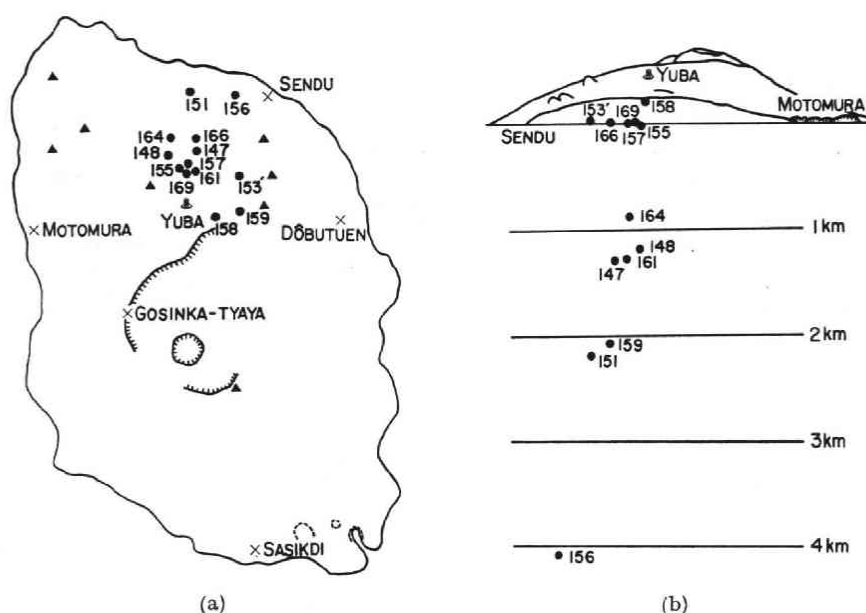


Fig. 26 Epicenters of earthquakes (after Takahashi and Nagata, 1939).

- (a) Horizontal distribution
(b) Vertical distribution

tion from the viewpoint of volcanology.

Fig. 25 shows a distribution of the Bouguer anomaly (Yokoyama and Tajima, 1957). Compared to the magnetic anomaly, the peak of the Bouguer anomaly shifts slightly toward the east, but both of them are similar as a whole.

In Oshima and its surroundings, a group of small earthquakes occurs at intervals of one or two years (Yokoyama, 1958). Takahashi and Nagata (1937) determined the foci of earthquake swarm. Fig. 26 shows the distribution of the earthquakes which occurred at about 1 to 2 km in depth on the northern side of the Oshima Island. This coincides with the place on the northern side of the magnetic sources A and B in Fig. 23. This area may be expected to become a crater in the future.

Results

(1) By aeromagnetic surveys at different heights, the magnetic structures of Oshima Volcano were found to be complicated by overlapping of several dipoles. And it became obvious that the anomaly sources were at 800 m to 4 km in depth under the surface.

(2) In spite of the observation of the scaler component of the total magnetic intensity, it becomes possible to study magnetically complicated structures such as in this volcano by means of aeromagnetic surveys. And it has been proved that this method is very effective.

(3) The distribution of the magnetic anomaly observed in the region from the crater to the southeastern part of Oshima Volcano is similar to that of the Bouguer

anomaly as a whole. This is due to the filling up of basaltic rocks with intense magnetization and high density.

(4) Near Yuba on the northern side of the crater, all of magnetic and Bouguer anomalies and seismic activities are coincidentally distributed around the same area with a fumarole. This area may become a new crater in the Oshima in the future.

3-2. *Hakone Volcano*

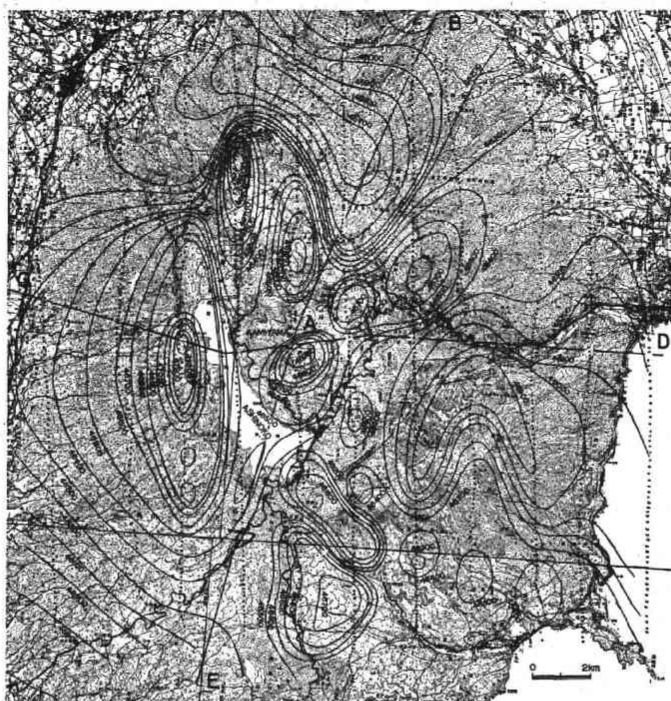
Hakone Volcano is a typical tripple volcano belonging to the same Fuji volcanic zone as Oshima Volcano and is located at about 30 km southeast of Mt. Fuji. The main part of the body is a gigantic strato-volcano with a central caldera which has diameters 11 km in the north-south and 10 km in the east-west respectively. The circular ridge surrounding this caldera is called the Old Somma which ranges in height from 800 to 1200 m. Mt. Kami-yama is one of the Central Cones and a strato-volcano (Kuno, 1953).

Aeromagnetic surveys were carried out over the area of the Hakone Caldera of 40 km in north-south diameter and 40 km in east-west diameter, centering around the Kami-yama (1438 m). The flight levels are 5000 ft and 6000 ft above the sea level. The magnetic intensity maps are shown in Figs. 27 and 28. Contour interval is 100 gammas. In Fig. 27, a high anomaly is extensively seen near the summit of Mt. Mikuni-yama belonging to the Old Somma. Some high anomalies are seen on the east side of the Old Somma. And the other anomalies due to the Central Cones are shown from the northwestern to the southeastern direction. On the northeastern part of the Caldera, a low anomaly extends broadly. In Fig. 28, the contour lines are simple in comparison with those in Fig. 27. Two aeromagnetic profiles (Fig. 29) at different altitudes including the topography are presented along the same courses as U.S.G.S. (1964) surveyed by a flux-gate magnetometer loaded on an aeroplane at 500 m over the terrain (Fig. 27). Two peaks at 5000 ft disappear at 6000 ft. In Fig. 29b, the anomalies at three different heights vary with height. The anomaly over the Old Somma is most distinct. On the eastern side of the Central Cones, a low anomaly extends.

An example (Fig. 30) for the analysis of the magnetic structure was calculated along a section (C-C' in Fig. 31), passing the Kami-yama, one of the Central Cones. For two magnetic anomalies, two prism-shaped models magnetized uniformly with the magnetic inclination of 50° were assumed and calculated by Bhattacharyya's formula (1964). The magnetic anomaly for the Kami-yama is caused by a dike at 1.0 km under the surface of the mountain with a magnetization of 6.4×10^{-3} (emu/cc), and the other one for the Daigadake is also caused by a dike at 0.5 km in depth with a magnetization of 8.4×10^{-3} (emu/cc). Further, the depth of the magnetic structure at the Old Somma became 7 km from the summit.

Discussion

Yokoyama (1964) carried out a gravimetric survey of Hakone volcano and proved the volcano as a typical caldera from its gravity anomaly. But the anomaly is not



COMPONENT : TOTAL INTENSITY UNIT : GAMMA HEIGHT : 5000 FT

Fig. 27 Total magnetic intensity over Hakone caldera at 5000 ft in height and traverse BAE and GAD of the aeromagnetic survey of U.S.G.S.



COMPONENT : TOTAL INTENSITY UNIT : GAMMA HEIGHT : 6000 FT

Fig. 28 Total magnetic intensity at 6000 ft in height.

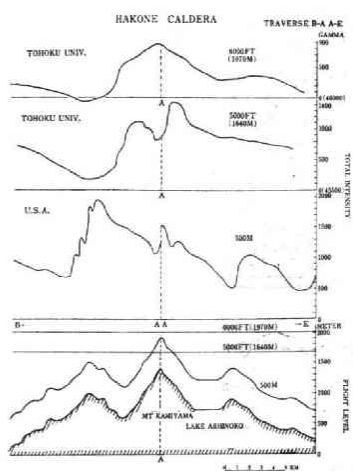


Fig. 29a Profiles along the traverse BAE.

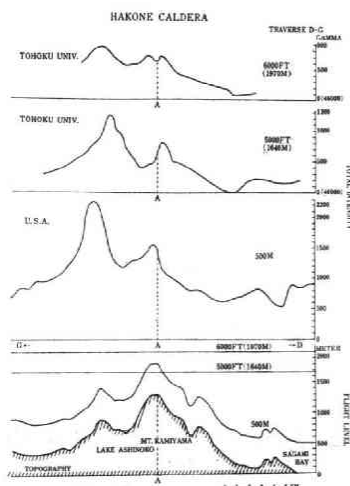


Fig. 29b Profiles along the traverse CAD.

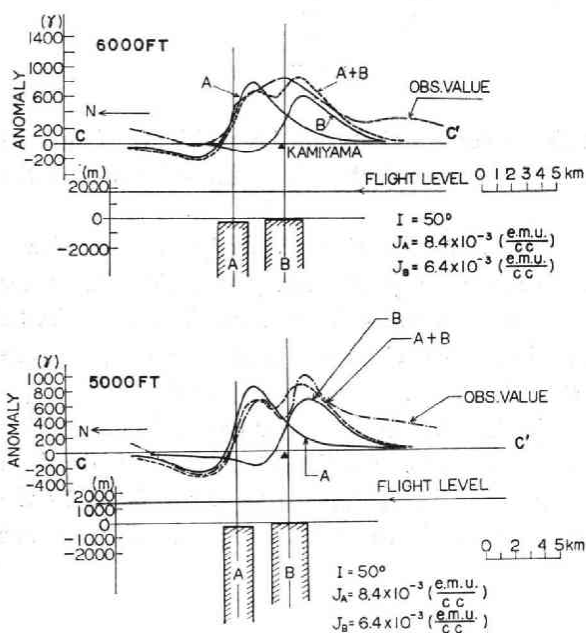


Fig. 30 Computed and observed anomaly along the line C-C'.

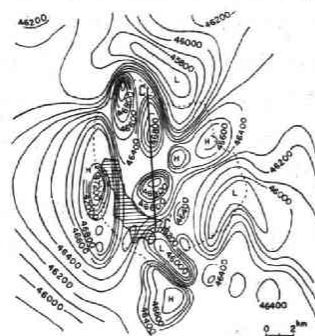


Fig. 31 Traverse C-C' used in interpretation of Fig. 30.

similar to the magnetic one in its feature. Therefore, it is thought that the magnetic anomaly sources in the Central Cones area are shallow in depth. Yukutake *et al.* (1960) surveyed the total intensity on the ground at the Kami-yama using a proton precession magnetometer. They found an anomaly on the mountain which reached 1000 gammas, with a strong magnetization of 2×10^{-2} (emu/cc). Although the 'Kin-toki-yama - Maku-yama' dislocation line had been discovered from a geological point of view, this line was confirmed by the aeromagnetic survey. The Central Cones

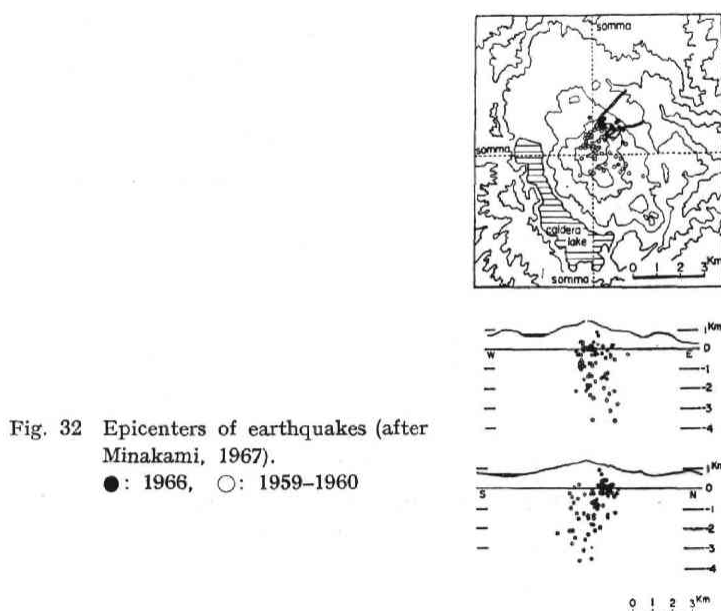


Fig. 32 Epicenters of earthquakes (after Minakami, 1967).
 ●: 1966, ○: 1959-1960

distributed along this line show that the volcanic activity has been violent. Hagiwara (1965) computed the autocorrelation and reported that such a line existed near the existing geological dislocation line.

Minakami (1960, 1967), has reported that the seismic activity in this volcano occurs around the Central Cones once in every few years. Many volcanic earthquakes took place during a period from September 1959 to April 1960, and in 1966. Fig. 32 shows the epicenters which are included within a circle of 1.5 km diameter, and the depth of the foci ranging from 1 to 6 km (1 to 2 km in nearly all cases) from the surface (A-type earthquakes by Minakami). The volcanic activity did not occur within the depth of 1 km from the surface of the volcano. On the other hand, the depth of the magnetic source around this area is about 1 km. This is the same depth as the foci. Therefore, the anomalous structure of the Central Cones in Hakone Volcano was well ascertained.

Results

(1) Distinctive features of the magnetic anomaly in Hakone Volcano were made clear: (a) A large positive anomaly extends on the north-south direction caused by the Somma lavas on the western side of the Lake Ashi. On the other hand, the anomalies on the eastern side of the lavas are small as a whole. (b) At the center of the volcano, several anomalies due to the Central Cones are distributed in a direction from the northwest to the southeast. (a) is caused by the dislocation line and (b) by the Central Cones along the line as mentioned above.

(2) The Bouguer anomaly shows a typical caldera. Magnetic anomaly does not necessarily show a caldera-like feature. From this result, it is estimated that the

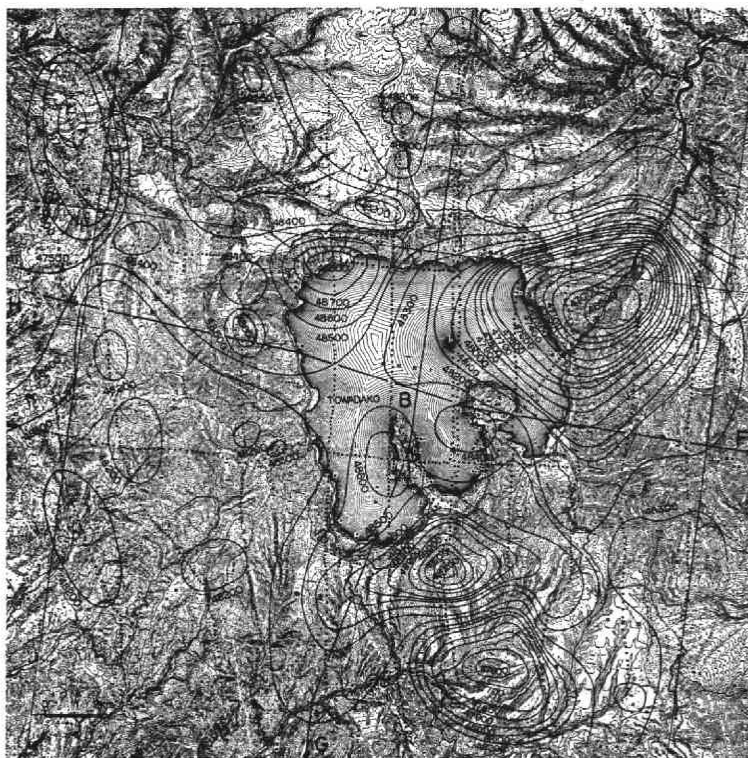


Fig. 33 Total magnetic intensity over Towada caldera at 4000 ft in height and traverses CBG and HBF of the flight coursed by U.S.G.S.



Fig. 34 Total magnetic intensity at 5000 ft in height and traverse AA'.

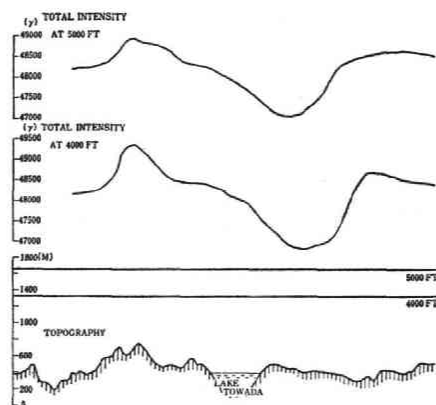


Fig. 35 An example of profile of the total intensity and topographical map.

Cones are situated at a shallow depth.

(3) The magnetic anomaly source of Mt. Kami-yama has a depth of about 1 km from the surface and the depth is close to that of the foci of earthquake swarms in the volcano.

3-3. Towada Caldera

Towada Caldera is a tripple volcano of the Krakatau type with a square-shaped lake of 10 km in each length. The basement rocks of the Caldera consist of welded tuff, propyrite and rhyolite on Tertiary. With these rocks as its basis, the first stage of the activity started with an eruption of rhyolitic dacite distributed mainly in Younger Pleistocene. The second stage was caused by andesitic basalt magma. Large amounts of pumice were also erupted. The third stage was extrusions of two lava domes (Mikura-yama and Gomon-iwa) situated along a dislocation line of NNW-SSE direction across the lake Towada. The fault forms an apparent dislocation line wall on the northern part (Kawano, 1939).

A square-like area with 25 km in each length around the Lake Towada called caldera topography from geological point of view was surveyed at two flight levels, 4000 ft and 5000 ft. Figs. 33 and 34 show the distribution of the total magnetic intensity. As shown in Fig. 33 there is a large low anomaly of about 10 km diameter having its center on the north-eastern shore of the Lake. Besides high and low anomalies at the distance of 2 km south of the Lake and a high anomaly on the north side of the Lake are observed. Therefore, the Lake is enclosed with these anomalies. Fig. 35 is a profile of the total intensity and topography along the NE-SW direction across the Lake. It is to be noted that this anomaly does not change with height nor reflect the surface topography. Vertical profiles at several altitudes along the two sections CBG and HBF (Fig. 33) are illustrated in Figs. 36 and 37. These curves are the total intensity at 500 m over the terrain (U.S.G.S., 1964), 4000 ft and 5000 ft above the sea level. These figures show: (a) several low anomalies correspond to the surface of the Lake and high anomalies to the rims. (b) these anomalies seem to reflect the surface

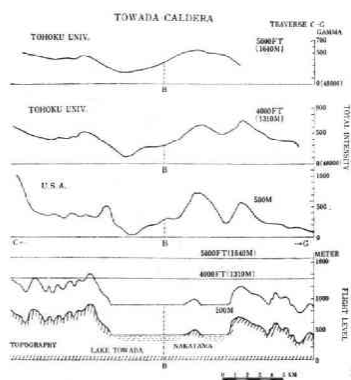


Fig. 36 Profiles of total intensity and topographical map along CBG.

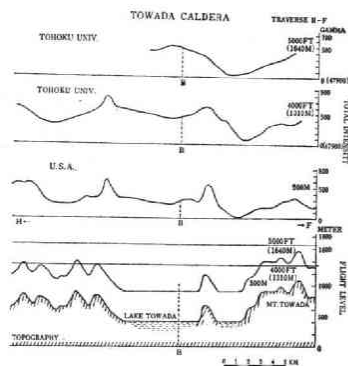


Fig. 37 Profiles of total intensity and topographical map along HBF.

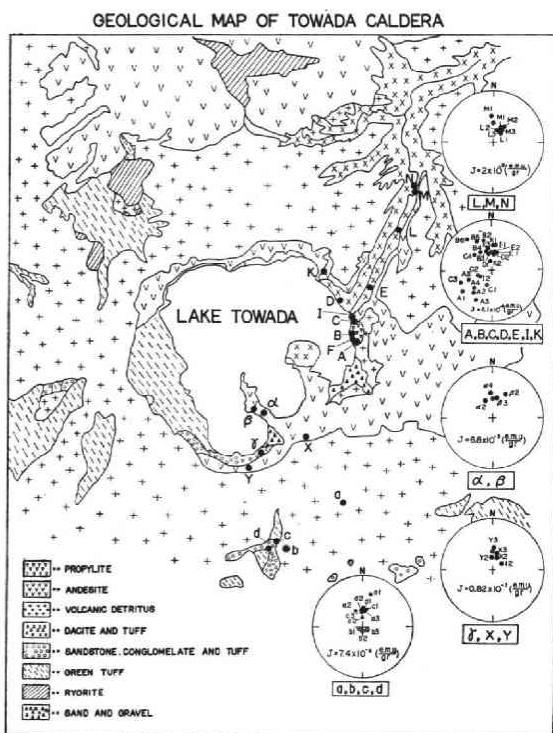


Fig. 38 Geological map of Towada Volcano (after Kawano, 1939) and the results of natural remnant magnetization of the samples from the area.



Fig. 39 Letters of line A-A' and B-B' used in interpretation in Fig. 40 and Fig. 41.

structure of the Caldera.

In order to explain these anomalies, magnetization of the rocks obtained from this caldera was actually measured. A stereographic projection of NRM (natural remnant magnetization) is shown on the right hand of Fig. 38. The NRM direction

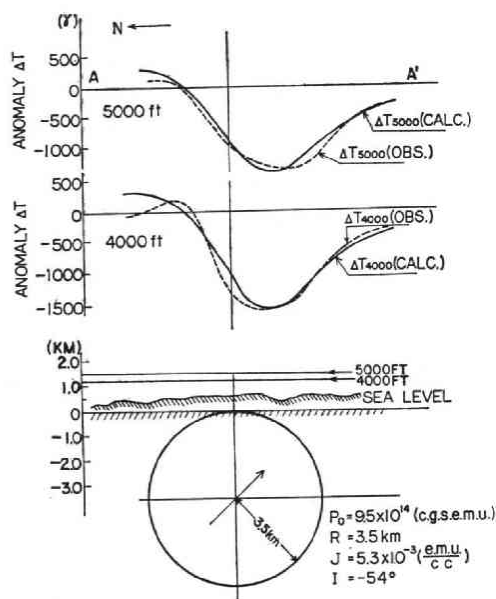


Fig. 40 Computed and observed anomaly along the line A-A'.

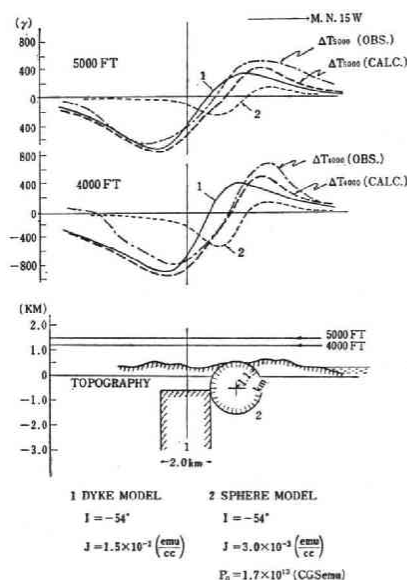


Fig. 41 Computed and observed anomaly along the line B-B'.

of pyrrhotite from Nenokuchi near the Oirase River (A and C) is reversed and its mean intensity is 5.1×10^{-4} (emu/gr), while that from Yasumiya at the south shore of the Lake is normal and its magnetization is 8.1×10^{-4} (emu/gr). Samples from Nakayama Peninsula have a normal direction and their magnetization is 6.8×10^{-3} (emu/gr) which is stronger in magnetization than that gathered in the two areas stated above. Analyses were carried out in these areas only (Fig. 39).

(a) Anomaly over the Oirase River

The values of n (denotes the form of the magnetized body) and d (its depth) were evaluated by the formula (3)': $n=3.1$, $d=4.7$. A dipole model of reverse magnetization with a value 5.3×10^{-3} (emu/cc) was assumed as the magnetic structure and the depth from the surface was obtained to be 4 km (Fig. 40). Although the calculated intensity is larger than the observed one, this anomaly seems to be interpreted sufficiently from the topography only.

(b) Anomaly over Yasumiya

The intensity of this anomaly does not change with the height level. Assuming the dike intruded from the underground as the magnetic structure (Fig. 41), the depth from the surface to the prism-shaped body with a square of 2 km in each length was estimated to be 1.1 km. The magnetization of the source was 1.5×10^{-3} (emu/cc). The residual obtained by subtracting the calculated value from the observed one was explained by assuming a dipole model with a reversed magnetization of 3.0×10^{-3} (emu/cc). This model was situated at the northern side of the former prism model and its depth from the surface was 1.1 km.

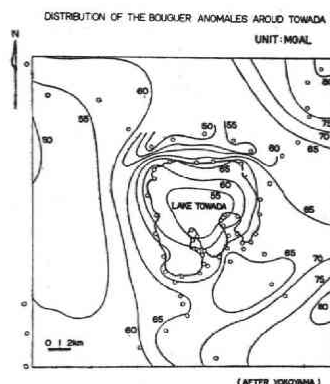


Fig. 42 Distribution of the Bouguer anomaly around Towada (after Yokoyama and Maki, 1964).

Discussion

Some examples of the magnetic anomalies in this caldera are presented in the preceding section. It is considered that the actual magnetic structure is not so simple as seen on the surface. Yokoyama (1964) reported that Towada Caldera showed a low gravity anomaly at the central part of the lake as the caldera was formed by collapse (Fig. 42). Whereas the magnetic anomalies only over and near the lake show such a feature as a caldera. Around the lake, however, the anomalies do not coincide with the gravity ones; especially there exists a large difference in such intense anomaly areas as Nenokuchi and Yasumiya.

It is well-known that during Miocene of Tertiary, the pole position of the geomagnetic field was reversed several times. Therefore, the interpretation of the magnetic anomalies would be easy if the age determination of the base rocks around the caldera were carried out.

Results

(1) Magnetic anomalies over Towada Caldera are considerable and show a characteristic feature as a caldera.

(2) A remarkable low anomaly over the Oirase River (about 1400 gammas at its peak value) which extends on the northeastern part of the lake shows the most striking feature and can be explained by a dipole model uniformly and reversely magnetized at 4 km in depth. The anomaly at Yasumiya can be interpreted by both a prism-shaped model and a sphere model with reversed magnetization at 1.1 km in depth.

(3) Gravity anomaly does not necessarily correspond to the magnetic one. Thus a precise age determination of the Tertiary rocks forming the basin of this caldera would make it easy to explain quantitatively these anomalies.

3-4. Onikobe Caldera

Onikobe area is known as a caldera-like topography with a volcanic basin. Arao-dake (Mt. Arao, 1984 m) and Takahiwa-yama (Mt. Takahiwa, 1796 m) are situated at the central part of this basin, and Arao (or Eai) River flows like a ring-shape around



Fig. 43 Total magnetic intensity over Onikobe caldera at 5000 ft in height and traverses BAD and EAC of the aeromagnetic survey by U.S.G.S.

these Central Cones. Around the river, somma-like peaks (1000~1260 m) are located, which are composed of granitic rocks, Tertiary sedimentary rocks and volcanic rocks, and the peaks (600~800 m) which embrace welded tuff are also located (Yamaoka, 1962).

Aeromagnetic survey was carried out over an area of 25 km in N-S diameter and of 15 km in E-W diameter centering the Arao. The flight level of seven courses along the geomagnetic meridian at interval of 2 km is 5000 ft above the sea level only. Fig. 43 shows a magnetic chart, in which a low anomaly is seen over the Mt. Arao and a higher anomaly over the Arao River on the western side of Mt. Arao.

The magnetic profiles obtained at 5000 ft above the sea level and 500 m over the terrain by U.S.G.S. (1964) including the topographic section are shown in Fig. 44 and Fig. 45. These are drawn along BAD and EAC as seen in Fig. 43. At the section EAC (Fig. 45), a magnetic low anomaly appears at the western side of Mt. Arao. From these profiles, Onikobe area is inclined to a caldera, though its tendency is not so remarkable.

Comparing with the other calderas, it is possible to estimate that this caldera has been constructed by a small scale eruption. Rikitake *et al.* (1965) carried out gravimet-

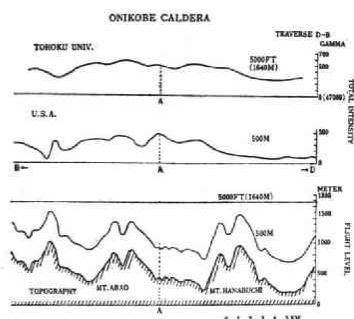


Fig. 44 Profiles of total intensity and topographical map along the traverse BAD.

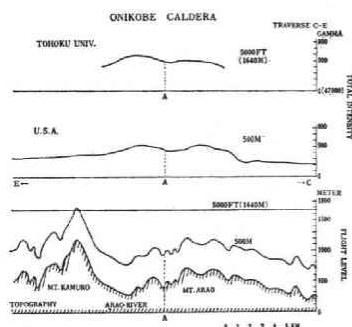


Fig. 45 Profiles of total intensity and topographical map along the traverse EAC.

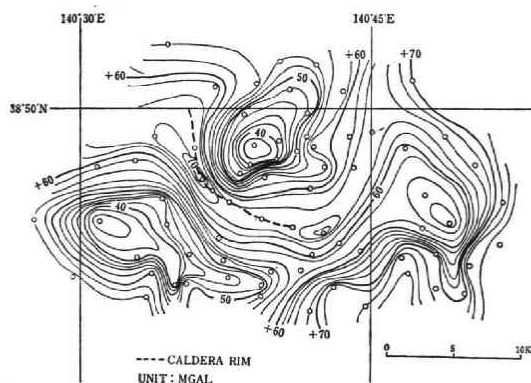


Fig. 46 Distribution of Bouguer anomaly in units of mgal (after Rikitake *et al.*, 1965).
----: the caldera rim.

ric and magnetic (vertical component) surveys over this area. A marked low gravity anomaly associated with the magnetic high anomaly was observed in the central part of this area (Fig. 46). They reported that the Onikobe area is a sort of caldera and seems to harmonize with the present geological view. But the author's result does not necessarily coincide with the vertical component anomalies.

The results obtained for this area are as follows.

(1) By aeromagnetic surveys, the informations showing the sufficient evidence of caldera-like topography have not necessarily been obtained. But it became obvious that the materials composing Mt. Arao are not only weak in magnetization, but also low in density.

(2) It is concluded that the center of the deep structure of this caldera is situated under the Arao River at the western side of the Mt. Arao.

4. Conclusions

1. Any volcano and caldera of Japan over which the aeromagnetic surveys were carried out, showed magnetic anomaly more or less. Oshima Volcano is composed of several complicated magnetic structures at depths from 1 to 4 km from the surface.

It was ascertained from the total magnetic surveys that Hakone Volcano and Towada Caldera have characteristic feature as a caldera, though these have been called so from the viewpoint of geology. Each of them also showed a dislocation line in the direction of NW to SE, along which several Central Cones erupted. Onikobe is a typical caldera with weak magnetic rocks for the most part. In order to clarify the mechanism of volcanic and orogenic activities, especially for Tertiary andesite composing the basin at Towada Caldera, age determination is needed. Further it is desired that actual structures of these volcanoes and calderas are determined by explosion seismology.

2. By aeromagnetic surveys at different heights using a proton magnetometer mounted in an aeroplane, the total intensity and its anomaly at each level were obtained and the data were used to analyze the magnetic structure of volcanoes and calderas. In this manner, the aeromagnetic survey is very effective to study the magnetic structure under the ground and also to observe an extensive area in a short time. It is not too much to say that the aeromagnetic survey is being used as a common method to investigate the geological structure (as an assistant means of a geological map).

Acknowledgements: The author expresses his hearty thanks to Prof. Y. Kato, Faculty of Technology, Tokai University, and to Prof. A. Takagi, the Aobayama Seismological Observatory, Faculty of Science, Tohoku University for their kind guidance and encouragement throughout this work. The author also wishes to express his appreciation to Dr. S. Utashiro, Hydrographic Office, Maritime Safety Agency, for providing the aeromagnetic map over Oshima Volcano at 3,000 ft height above the sea level. He is also grateful to Prof. I. Aoyama, Faculty of Technology, Tokai University, and to Dr. Y. Mori, Institute of Earth Science, Miyagi University of Education for their kind assistance. The Author wishes to express his sincere thanks to the staff member of All Nippon Airways for their assistance in surveys and to Nippon Electric Company which collaborated in the development of the equipment.

Acknowledgement is also made of the financial support for aeromagnetic surveys through a grant from the Japan Society for Promotion of Science as part of the U.S.-Japan Cooperative Science Program.

REFERENCES

- Allan, T.D., 1965: A magnetic survey off the coast of Portugal. *Geophysics*, **30**, 411-417.
Bhattacharyya, B.K., 1964: Magnetic anomalies due to prism-shaped bodies with arbitrary polarization. *Geophysics*, **29**, 517-531.
Hagiwara, Y., 1965: Analysis of the results of the aeromagnetic survey over volcanoes in Japan (I). *Bull. Earthq. Res. Inst.*, **43**, 529-538.
Hartman, R.R., D.J. Teskey, and J.L. Friedberg, 1971: A system for rapid digital aeromagnetic interpretation. *Geophysics*, **36**, 891-918.
Henderson, R., and I. Zietz, 1949: Computation of second vertical derivatives of geomagnetic fields. *Geophysics*, **14**, 508-518.
Hood, P., and D.J. McClure, 1965: Gradient measurements in ground magnetic prospecting. *Geophysics*, **30**, 403-410.

- Kato, Y., T. Matsuo, and A. Takagi, 1962: Aeromagnetic surveys over the Oshima Island. *Sci. Rep. Tohoku Univ. Ser. 5, Geophys.*, **14**, 65-80.
- Kawano, Y., 1939: Chemical study of the eruptive materials on Towada Volcano. *Jour. Petr. Min. Econ. Geol.*, **22**, 223-239.
- Kuno, H., 1953: Kazan and Kazan-gan (Volcano and Volcanic Rocks). Iwanami-shoten, p. 255.
- Kuno, H., 1962: Guide-Book for Excursions. Volcanological Society of Japan, p. 84.
- Minakami, T., 1960: Fundamental research for predicting volcanic eruptions (Part I). *Bull. Earthq. Res. Inst.*, **38**, 497-544.
- Minakami, T., 1967: Volcanic earthquakes. *Zisin (J. Seism. Soc. Japan)* Special Issue, **20**, 177-181.
- Rikitake, T., 1951: The distribution of magnetic dip in Oosima (Oo-sima) Island and its change that accompanied the eruption of Volcano Mihara. 1950, *Bull. Earthq. Res. Inst.*, **29**, 161-190.
- Rikitake, T., I. Yokoyama, A. Okata, and Y. Hishiyama, 1951: Geomagnetic studies of Volcano Mihara. The 3rd paper (Magnetic survey and continuous observation of changes in geomagnetic declination). *Bull. Earthq. Res. Inst.*, **19**, 583-614.
- Rikitake, T., H. Tajima, S. Izutsuya, Y. Hagiwara, K. Kawada, and Y. Sasai, 1965: Gravimetric and geomagnetic studies of Onikobe area. *Bull. Earthq. Res. Inst.*, **43**, 509-528.
- Slack, H.A., V.M. Lynce, and L. Langn, 1967: The geomagnetic gradiometer. *Geophysics*, **32**, 877-892.
- Smellies, D.W., 1956: Elementary approximation in aeromagnetic interpretation. *Geophysics*, **21**, 1021-1040.
- Takahashi, R., and T. Nagata, 1939: On the earthquake swarm occurred in Oshima Island at June 18th, 1938. *Zisin (J. Seism. Soc. Japan)*, **2**, 161-167.
- U.S.G.S., 1964: Aeromagnetic survey over the calderas in Japan. Review Meeting on Combined Aero-Gravity Studies of Calderas in Japan, U.S.-Japan Cooperative Science Program. Hokkaido, Japan.
- Vacquier, V., and S. Uyeda, 1967: Paleomagnetism of nine seamounts in the western Pacific and of three volcanoes in Japan. *Bull. Earthq. Res. Inst.*, **45**, 815-848.
- Wickermann, W.E., 1954: The Gulf airborne magnetic gradiometer. *Geophysics*, **19**, 111-123.
- Yamaoka, K., and A. Shimada, 1962: On the diatom earth at the Onikobe, Narugo-machi, Miyagi Prefecture, Mineral Resources for Industry in Northeastern Japan (Part II). 259-262.
- Yokoyama, I., 1957: Geomagnetic anomaly on volcanoes with relation to their subterranean structure. *Bull. Earthq. Res. Inst.*, **35**, 327-357.
- Yokoyama, I. and H. Tajima, 1957: A gravity survey on Volcano Mihara Island by means of a Worden Gravimeter. *Bull. Earthq. Res. Inst.*, **35**, 23-61.
- Yokoyama, I., 1958: Review of geophysical researches on Volcano Oshima. *Kazan (J. Volcan. Soc. Japan)*, **3**, 39-69.
- Yokoyama, I., and T. Maki, 1964: Preliminary report on a gravimetric survey on Towada Caldera, Tohoku District, Japan. *Jour. Fac. Sci. Hokkaido Univ. Ser. 7*, **2**, 251-258.
- Yokoyama, I., and T. Saito, 1964: Preliminary report on a gravimetric survey on Volcano Hakone, Japan. *Jour. Fac. Sci. Hokkaido Univ. Ser. 7*, **2**, 239-245.
- Yukutake, T., and I. Tanaoka, 1960: Magnetic survey on Hakone Volcano by use of a proton magnetometer. *Bull. Earthq. Res. Inst.*, **38**, 41-54.